2004-1-523

Pergamon

Geochimica et Cosmochimica Acta, Vol. 68, No. 21, pp. 4319–4333, 2004

0016-7037/04 $30.00 + .00

doi:10.1016/j.gca.2004.01.020

Geochemistry of soils of King George Island, South Shetland Islands, West Antarctica: Implications for pedogenesis in cold polar regions

YONG IL LEE,[1,*] HYOUN SOO LIM,[1] and HO IL YOON[2]

[1]School of Earth and Environmental Sciences, Seoul National University, NS 80, Seoul 151-747, Korea
[2]Polar Research Center, Korea Ocean Research and Development Institute, Ansan P.O. Box 29, 425-600, Korea

(*Received August* 27, 2003; *accepted in revised form January* 15, 2004)

Abstract—Fine fractions of soils on the Barton Peninsula, King George Island, West Antarctica have been forming during the last 6000 yr since the last deglaciation. Texturally, they are mostly composed of mineral and rock fragments with some volcanic ashes, which are also indicated by geochemical compositions representing for the nonclay silicate minerals and low values of chemical index of alteration. No significant changes are observed in major- and trace element abundances. Such geochemical characteristics suggest that chemical weathering of bedrocks on the Barton Peninsula seems insignificant and that the soils are composed of physically weathered mineral and rock fragments which are mixed with eolian additions of volcanic ashes and Patagonian dusts. Chondrite-normalized rare earth element (REE) distribution patterns of the Barton Peninsula soils are slightly different from those of bedrocks, indicating that the REE abundances and characteristics were influenced by eolian additions. Mixing calculations, which mass-balance the REEs, suggest that volcanic ashes blown from Deception Island were the major eolian contributor, followed by atmospheric dusts sourced from Patagonia, South America. Even in the warmer and humid climatic conditions in the maritime Antarctic region, the chemical weathering of bedrocks appears to be insignificant, probably due to the relatively short duration of weathering since the last deglaciation. *Copyright © 2004 Elsevier Ltd*

1. INTRODUCTION

In Antarctica, chemical weathering is not sufficiently important to cause major change in bulk composition of rocks and soils (Kelly and Zumberge, 1961). The general conclusions on soil formation in Antarctica are that chemical weathering processes operate only to a very limited extent and that rock disintegration and soil formation are brought about largely by physical processes. The vegetation is restricted to mosses, lichens and algae because of the severe environments (Seppelt and Broady, 1988). Higher plants do not occur because of low temperatures and strong winds (Pickard, 1986). However, in the maritime Antarctica, covering parts of the Antarctic Peninsula and the offshore islands, the climate is warmer and much greater quantities of free water are available. Soils in this part of the Antarctica are characterized by much greater predominance of cryoturbic processes as evidenced by the presence of patterned ground (Campbell and Claridge, 1987). Recently, it was reported that the main limitation on freeze-thaw weathering is not thermal but rather moisture (Hall, 1997), and that in ice-free areas close to the coastal regions soil formation and chemical weathering occurs to a greater extent than previously thought (Blume et al., 1997; Beyer et al., 2000). In addition, although the reactions are probably slow in Antarctic conditions, chemical weathering was suggested as the main process contributing magnesium, calcium and carbonate ions into the salt deposits (Keys and Williams, 1981). Seabirds' organic matter mostly affects the soil formation in these areas.

Chemical compositions of soils vary as a function of various soil-forming processes. To interpret the soil-forming processes and factors operating at the soil site properly one needs to test parent-material uniformity. One source of nonuniformity is the influence of allogenic materials, which may be important where physical weathering is more significant than the chemical weathering such as in Arctic and Antarctic regions as well as cold desert regions. These areas are characterized by strong wind activity, resulting in mixing of in situ soils with eolian input materials. Eolian dust deposits are prominent in many parts of the world, both on continents and in oceans (Pye, 1987), and play an important role in the formation of soils (Simonson, 1995, and references therein) and deep-sea sediments (Rea et al., 1985). Eolian dust can also affect the composition of ice in glaciers (Waghenbach and Geis, 1989; De Angelis and Gaudichet, 1991). It is now well established from ice-core studies that the concentration of dust in the Antarctic atmosphere increased by a factor of 10–100 during Quaternary glacial maxima (e.g., Petit et al., 1999). If there are volcanic eruptions, volcanic ashes are also transported through the eolian transport (Basile et al., 2001). The proportion of the eolian additions in the soils depends on the wind speed or direction. Examples of eolian input to the soils developed in the ice-free areas of Antarctica were described by Beyer et al. (2000) and Jeong and Yoon (2001).

Chemical characteristics of soils in the offshore islands of the maritime Antarctic region have not been studied before although this region has a higher potential for chemical weathering because of its warmer and more humid climate than other parts of Antarctica (e.g., Campbell and Claridge, 1987). Instead of studying total changes in the soil profile, this study focuses on characterizing the surface soils in this maritime Antarctic region. Soils in this region are suggested to have formed since the last deglaciation, ca. 9500–6000 yr BP. By studying geochemical characteristics of the reactive finer-grained soil fractions we try to determine the degree of chemical weathering, and the contribution of allogenic materials including eolian

* Author to whom correspondence should be addressed (lee2602@plaza.snu.ac.kr).

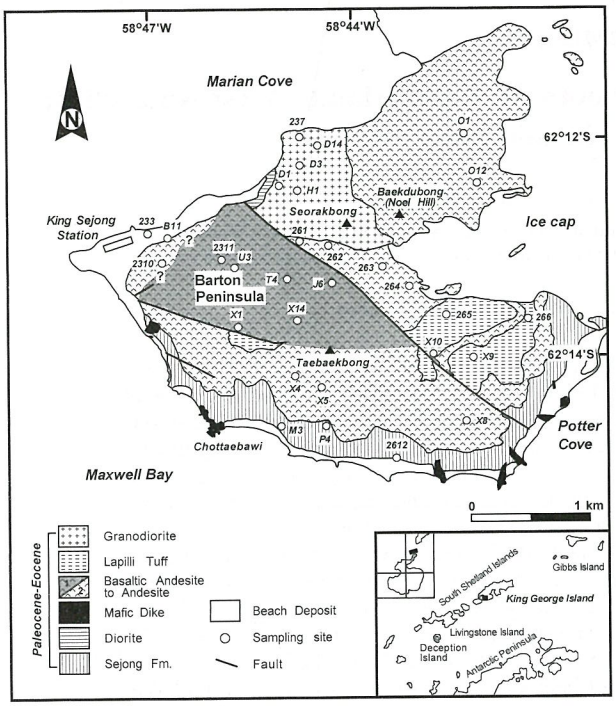

Fig. 1. Geological map of the Barton Peninsula, King George Island, West Antarctica. The inset shows the location of King George Island. The numbered open circles in the geological map represent the soil sampling sites.

additions to the soils. The results of this study may contribute to the understanding of pedogenesis in cold polar regions.

2. GEOLOGICAL SETTING

The South Shetland Islands, located offshore the Antarctic Peninsula (Fig. 1), are calc-alkaline island arcs, separated from the Antarctic Peninsula by the young marginal basin, the Bransfield Strait. King George Island is situated in the middle of the South Shetland Islands. The study area, the Barton Peninsula, is the southwestern part of King George Island (Fig. 1). Most of King George Island is covered with glaciers and outcrops are exposed only along the shorelines in restricted areas. The Barton Peninsula has a rugged topography with a wide and gentle slope in the central belt having elevations of 90–180 m above sea level. Marian and Potter coves (Fig. 1) are fjords into which outlet glaciers currently calve, producing icebergs. Permafrost is known to be present 1 m below the surface (Jeong and Yoon, 2001), and thus the active layer on the Barton Peninsula may be approximately 1 m thick.

The geological map of the Barton Peninsula is shown in Figure 1. The lowermost lithostratigraphic unit is the Sejong Formation (Yoo et al., 2001), which is largely composed of volcaniclastic constituents with maximum thickness of ~100 m. It is dated to be Late Paleocene to Eocene based on plant fossil leaves (Chun et al., 1994). Mafic to intermediate volcanic lavas overlying the Sejong Formation are widely distributed in the peninsula. They are mostly plagioclase-phyric or plagioclase- and clinopyroxene-phyric basaltic andesite to andesite with rare massive andesite (Lee et al., 2001). Several units of thick-bedded lapilli tuffs are intercalated with lava flows. Although the eruption ages are difficult to constrain, it is likely that most lavas were erupted during Paleocene to Eocene (Pankhurst and Smellie, 1983; Smellie et al., 1984; Kim et al., 2000; Hur et al., 2001). A granodiorite stock with minor fine-grained diorite occurs in the central northern Barton Peninsula. Previous age data indicate that this pluton was intruded during the Eocene (Park, 1989; Lee et al., 1996; Kim et al., 2000).

The basaltic andesite in the Barton Peninsula can be distinguished into two types, BA1 and BA2, based on the characteristics of rare earth elements (REEs), especially the degree of Eu anomaly and total REE content (Yeo et al., 2004; Fig. 1). BA1 basaltic andesites belong to the tholeiitic basalt to basaltic andesite with positive Eu anomalies (av. $Eu/Eu^* = 1.11$), whereas BA2 basaltic andesites belong to transitional basaltic andesite to andesite with negative Eu anomalies (av. $Eu/Eu^* = 0.86$). The BA1 volcanic rocks are distributed with a wedge shape in the central western part of the peninsula, which forms the gently inclined area between two high peaks (Fig. 1). The BA2 volcanic rocks are more widely distributed in the peninsula, and are in contact with the BA1 rocks along strike slip faults.

Pervasive hydrothermal alterations are observed in the northern part of the peninsula (east of the granodiorite), caused by the granodiorite intrusion. Four hydrothermal alteration types are recognized; prophyllic, phyllic, argillic and advanced argillic (Hwang and Lee, 1998; Hur et al., 2001). The altered BA2 rocks are composed of quartz, pyrite, and clay minerals such as illite, kaolinite, and pyrophyllite (Park, 1990).

3. PALEOCLIMATE

King George Island has a cold oceanic climate. Current climatic data for the study area recorded at the King Sejong Station for 9 yr (1988–1996) show an average annual temperature of −1.8°C, relative humidity of 89%, precipitation of 437.6 mm, and wind velocity of 7.9 m/s, with major directions of northwest and southwest (Lee et al., 1997). The climate is warmer and more humid than in other Antarctic areas. Thus, the study area possesses a cold and humid morphoclimatic system with a relatively high availability of water in the summer (soil and atmosphere wet) and frequent freeze-thaw cycles. Such features favor periglacial processes, and the presence of a usually saturated active layer in summer.

Paleoclimate and deglaciation history of the South Shetland Islands have been studied using various methods such as absolute age dating, oxygen isotope compositions, and diatom analysis of lake or marine sediments (Barsh and Mäusbacher, 1986; Sugden and Clapperton, 1986; Björck et al., 1991; Yoon et al., 2000). Overall data imply that the deglaciation of King George Island occurred ~6000 yr ago and that a climatic optimum occurred between ca. 4000 and 3000 yr BP in the South Shetland Islands (Björck et al., 1991; Yoon et al., 2000).

4. METHODS

A total of 30 surface soil samples were collected from the uppermost 10 cm of the active layer in the soil on the Barton Peninsula. Soils on altered bedrocks were avoided. Soil samples were dried and impregnated with epoxy under vacuum and thin sections were made. Soil samples were subdivided into two parts by a 230-mesh sieve, and finer fractions (< sand size) and coarser rock debris were separately pow-

dered in an agate motar and fused-glass beads were prepared for major element analysis by a Philips PW244 model X-ray fluorescence spectrometer. Total Fe content is reported as Fe_2O_3. Loss on ignition (LOI) was measured by weighing before and after 1 h of calcinations at 1000°C. The errors for geochemical sedimentary standards (Sco-1 and Ipt-61) are within ±10% for major elements. Trace elements and rare earth elements concentrations were determined using a Jobin Yvon 138 Ultrace inductively coupled plasma atomic emission spectrometer (ICP-AES) and a Perkin Elmer Elan 6100 inductively coupled plasma mass spectrometer (ICP-MS). Analytical precision for both trace elements and REEs is better than 5%. For major, trace, and rare earth elements concentrations three analyses were made for each sample and averaged. All major, trace, and rare earth elements were analyzed at the Korea Basic Science Institute. The total organic carbon and CO_2 contents were measured by a UIC CM5012 CO_2 Coulometer.

5. RESULTS

5.1. Soil Distribution

Because the Barton Peninsula is a narrow area, 4 km wide, and has generally been covered by a rather stagnant ice cap (Lee, 1992), debris from glacial erosion has not been transported great distances. Therefore, rock fragments in surface soils generally reflect the lithology of the basement rocks due to the breakage of bedrocks and subsequent particle size reduction by physical weathering, which is consistent with the observation of Jin et al. (1989).

In the Barton Peninsula an active layer is formed when the snow dissolves and moistens the soils during the summer period. Much of the surfaces in the central belt having gentle slope are characterized by active polygonal patterned ground. Half of the sampling sites are characterized by patterned ground with well developed stone polygons, generally of constant size, ranging from 1.2 m to 2.2 m in diameter, but stone stripes and solifluction lobes are poorly developed, which suggests that most of the soils are developed in situ. The boundaries of the polygonal features are marked by raised rims composed of angular pebbles and cobbles. The inner borders of the polygons are commonly vegetated by lichens, *Usnea aurantico-atra*. However, in the topographically controlled areas, some mixtures of surface soils are expected due to solifluction and wind activity.

Soils are unsorted and composed of mineral and rock fragments derived from the bedrock and volcanic ashes. The ash particles are mostly pumice glass shards both unaltered and altered (Fig. 2), having a basaltic andesite and partly basalt composition (Jwa and Kim, 1991). Petrographic observation shows that pumice shards in the soils are most abundant in the western region of the peninsula (up to 20%). Jeong and Yoon (2001) interpreted that they were blown from Deception Island located ~130 km southwest of King George Island (Fig. 1). The most recent activity was an eruption within the caldera of Deception Island in 1969 (Orheim, 1972), which formed a new debris cone and destroyed several scientific stations.

5.2. Major Elements

Major element data are given in Table 1. Loss on ignition (LOI) varies from 1.6% to 9.4%, reflecting variable amounts of carbonate, hydrous phases like clays, and organic matter. In SiO_2 vs. Al_2O_3 and SiO_2 vs. CaO diagrams (Fig. 3), the Barton Peninsula soils show a compositional variability. For example,

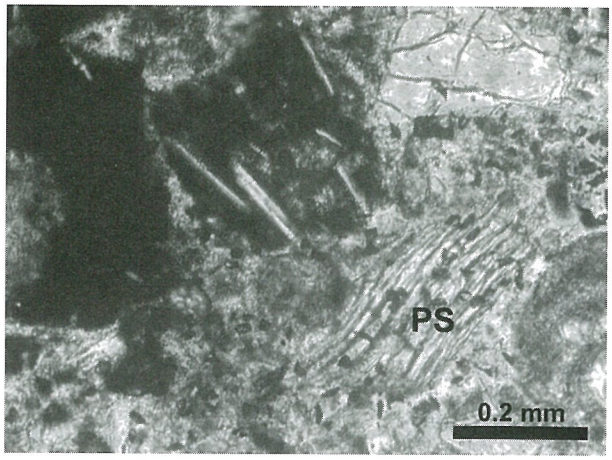

Fig. 2. Photomicrograph of soil sample showing rock and mineral fragments. Also shown are pumice shards (PS) that are partly altered to clay minerals.

SiO_2 contents vary from 47.5% to 65.7% and Al_2O_3 from 15.7% to 21.5%. As expected, there is a moderate negative correlation between SiO_2 and Al_2O_3 (correlation coefficient, $r = -0.55$). Also, there exist good correlations between SiO_2 and Fe_2O_3 ($r = -0.85$) and between SiO_2 and TiO_2 ($r = -0.81$).

Based on bedrock type, Barton Peninsula soils are subdivided into four suites; soils on granodiorite (S-GD), soils on basaltic andesite (S-BA), soils on lapilli tuff (S-LT), and soils on the Sejong Formation (S-SJ). Soils on basaltic andesite are further subdivided into two subsuites, S-BA1 developed on BA1 volcanic rocks and S-BA2 on BA2 volcanic rocks. The S-BA1 and S-BA2 can be differentiated in the cross-plot of SiO_2 vs. CaO, Al_2O_3 vs. K_2O, and Al_2O_3 vs. CaO except for one S-BA1 sample (U3) (Fig. 3). Compared to the S-BA2, S-BA1 has lower contents of SiO_2 and K_2O, but higher contents of CaO and TiO_2.

Total organic carbon (TOC) content of the Barton Peninsula soils ranges from 0.06% to 2.97% with an average of 0.76% (Table 1). S-SJ contains the highest average TOC content of 1.7%, followed by S-BA1 (1.4%) and the lowest TOC in the S-GD (0.2%). LOI content is well correlated with TOC content ($r = 0.83$), indicating that the LOI value represents the organic matter content.

5.3. Trace Elements and Rare Earth Elements

Average concentrations of Rb, Sr, and Ba range from 18.7 (S-BA1)–51.3 (S-LT) ppm, 287.0 (S-SJ)–366.5 (S-BA1) ppm, and 164.8 (S-BA1)–385.7 (S-LT) ppm, respectively (Table 2). As expected, S-GD contains relatively higher Rb (48.9 ppm), Sr (322.1 ppm), and Ba (359.1 ppm) contents than other soil suites, whereas S-GD have slightly lower contents of transition metals such as Cr (14.8 ppm), Co (17.3 ppm), Ni (8.9 ppm), and V (148.4 ppm). For high field strength elements, no general trend is observed among different soil suites.

REE data for the five soil suites analyzed are also given in Table 2 and average values are shown as chondrite-normalized patterns in Figure 4. Although REE data are somewhat variable,

Table 1. Major element compositions of soil and lithic fragment samples from the Barton Peninsula.

Sample	Al_2O_3	CaO	Fe_2O_3	K_2O	MgO	MnO	Na_2O	P_2O_5	SiO_2	TiO_2	LOI	Total	TOC	CO_2	CIA	ICV
Soils on granodiorite (S-GD)																
237	17.51	2.30	7.51	2.13	2.90	0.12	2.42	0.20	60.17	0.73	4.05	100.03	0.15	nd	63.7	1.0
D1	18.96	4.85	8.03	1.40	3.47	0.14	3.46	0.18	56.28	0.84	2.49	100.10	0.15	nd	54.9	1.2
D3	17.64	2.19	5.72	2.68	2.30	0.11	2.58	0.21	61.87	0.71	3.77	99.79	0.20	0.03	62.5	0.9
D14	15.65	3.09	4.50	3.01	1.72	0.10	3.69	0.14	65.72	0.55	1.57	99.75	0.18	nd	51.7	1.1
HI	16.12	3.47	9.69	1.82	1.75	0.35	3.34	0.22	57.97	0.91	4.00	99.65	0.36	nd	54.9	1.3
av.	17.17	3.18	7.09	2.21	2.43	0.17	3.10	0.19	60.40	0.75	3.18	99.86	0.21		57.5	1.1
SD*	1.32	1.08	2.02	0.65	0.75	0.10	0.56	0.03	3.65	0.14	1.10	0.19	0.09		5.25	0.15
Soils on basaltic andesite 1 (S-BA1)																
2311	18.40	5.33	9.47	0.74	3.66	0.15	2.73	0.44	48.23	1.53	9.37	100.04	2.90	0.05	57.1	1.3
X1	19.49	8.06	9.84	0.58	3.39	0.18	2.98	0.21	48.22	1.26	5.99	100.20	0.98	nd	49.8	1.3
X14	17.78	6.51	9.16	0.89	3.89	0.16	3.62	0.29	52.41	1.52	3.87	100.10	0.56	nd	49.6	1.4
J6	19.35	5.07	9.35	0.82	3.56	0.15	2.98	0.70	47.53	1.49	9.24	100.25	2.17	nd	59.2	1.2
T4	18.14	6.22	9.92	0.71	3.63	0.15	3.36	0.36	49.42	1.58	6.75	100.25	1.42	nd	52.0	1.4
U3	21.45	1.74	7.54	2.10	2.83	0.08	1.09	0.38	54.62	0.82	7.19	99.83	0.32	nd	77.3	0.8
av.	19.10	5.49	9.21	0.97	3.49	0.14	2.79	0.40	50.07	1.37	7.07	100.11	1.39		57.5	1.2
SD	1.33	2.12	0.87	0.56	0.36	0.03	0.89	0.17	2.82	0.29	2.07	0.16	0.99		10.45	0.25
Soils on basaltic andesite 2 (S-BA2)																
X4	19.50	1.26	9.03	1.77	1.32	0.17	3.09	0.29	56.52	1.10	5.76	99.80	0.27	nd	69.4	0.9
X5	18.46	5.17	9.96	1.24	2.96	0.18	3.49	0.31	50.78	1.49	6.04	100.09	1.20	nd	54.0	1.3
X8	19.30	3.11	9.36	1.93	3.40	0.19	2.83	0.39	50.79	1.23	7.36	99.90	1.50	nd	62.7	1.1
O1	19.10	4.75	8.21	1.90	3.34	0.14	2.02	0.17	54.78	0.78	4.62	99.82	0.07	0.01	58.5	1.1
O12	18.08	3.84	5.69	1.56	2.21	0.10	3.94	0.21	60.22	1.12	2.80	99.78	1.03	nd	55.2	1.0
261	19.55	3.83	9.37	1.07	4.02	0.18	2.54	0.27	51.77	0.90	5.92	99.42	0.46	nd	62.7	1.1
262	18.85	4.07	8.72	1.08	3.96	0.15	2.49	0.27	53.85	0.90	5.73	100.06	0.30	nd	61.1	1.1
263	19.31	4.39	7.87	1.13	3.70	0.14	2.87	0.32	52.58	1.01	6.47	99.80	0.84	nd	59.5	1.1
264	17.70	3.95	7.86	1.62	2.59	0.20	2.99	0.35	57.15	0.99	4.69	100.08	0.32	nd	57.6	1.1
233	16.54	4.29	6.94	1.66	2.32	0.11	3.23	0.18	61.30	0.76	2.71	100.04	0.38	nd	53.4	1.2
2310	16.63	4.11	7.51	1.59	2.44	0.11	3.00	0.18	61.11	0.76	2.61	100.07	0.15	nd	54.8	1.2
B11	17.47	4.30	6.92	1.59	2.59	0.11	3.41	0.17	60.18	0.75	2.45	99.94	0.06	nd	54.2	1.1
av.	18.38	3.92	8.12	1.51	2.90	0.15	2.99	0.26	55.92	0.98	4.76	99.90	0.55		58.6	1.1
SD	1.08	0.98	1.24	0.31	0.81	0.03	0.51	0.08	4.06	0.23	1.72	0.19	0.48		4.78	0.10
Soils on lapilli tuff (S-LT)																
265	17.43	1.70	8.49	2.00	2.67	0.18	2.07	0.28	56.12	1.03	5.14	97.10	0.15	0.01	68.6	1.0
266	18.18	2.50	9.43	2.07	3.24	0.17	2.74	0.28	54.20	1.22	5.98	100.01	0.92	nd	63.1	1.2
X9	17.98	1.77	7.42	2.58	2.54	0.16	2.50	0.35	59.44	0.96	3.81	99.52	0.15	0.19	67.0	1.0
X10	18.25	2.52	8.25	1.81	2.87	0.16	3.13	0.33	56.44	1.20	4.73	99.69	0.48	0.00	62.6	1.1
av.	17.96	2.12	8.40	2.12	2.83	0.17	2.61	0.31	56.55	1.10	4.92	99.08	0.43		65.3	1.1
SD	0.37	0.45	0.83	0.33	0.31	0.01	0.44	0.04	2.17	0.12	0.90	1.33	0.36		2.93	0.08
Soils on the Sejong Fm. (S-SJ)																
M3	19.79	2.87	9.62	1.72	2.64	0.15	2.33	0.52	52.54	1.26	6.65	100.08	0.90	nd	67.2	1.0
P4	17.60	3.14	8.54	1.81	2.26	0.15	3.31	0.38	55.43	1.28	6.02	99.91	1.17	0.03	59.2	1.2
2612	16.61	5.12	10.03	1.38	2.96	0.15	2.81	0.58	49.83	1.42	9.18	100.07	2.97	nd	54.2	1.4
av.	18.00	3.71	9.40	1.64	2.62	0.15	2.81	0.49	52.60	1.32	7.28	100.02	1.68		60.2	1.2
SD	1.63	1.23	0.77	0.23	0.35	0.00	0.49	0.10	2.80	0.09	1.67	0.09	1.13		6.56	0.20

all but S-BA1 display a single general trend based on curve shape and degree of Eu anomaly (Fig. 4). They have small negative Eu anomalies (Eu/Eu* = 0.73~0.89) and some fractionation of the LREEs and HREEs [average (La/Sm)n = 2.0~2.2 and average (Gd/Yb)n = 2.1~2.4, respectively]. Average total REE contents are variable in these soils: S-GD 134.8 ppm, S-BA2 134.9 ppm, S-LT 170.3 ppm, and S-SJ 125.9 ppm. S-BA1 displays less fractionation of the LREEs [average (La/Sm)n = 1.7] and HREEs [average (Gd/Yb)n = 1.7] and no Eu anomaly (Eu/Eu* = 1.0). Also, S-BA1 has the lowest total REE content (average 94.3 ppm). All soil samples show very slight negative Ce anomaly (average Ce/Ce* = 0.91~0.97) (Fig. 4).

6. DISCUSSION

Most of Antarctica has an extremely cold and arid climate, and consequently, Antarctic soils show many similarities with desert soils in other parts of the world including accumulation of soluble salts in the soil profile (Claridge and Campbell, 1977). However, in the maritime Antarctic region precipitation exceeds evaporation for much of the year, thus little or no accumulation of soluble salt is expected, which is evidenced by the chemical composition (Table 1).

6.1. Mineralogy of Soils: Primary vs. Secondary

The chemical composition of soils can be used to suggest the mineralogy of the soils, such as primary minerals or secondary weathering minerals. One approach to estimate the degree of chemical weathering is to use the Index of Compositional Variability (ICV)[ICV = (Fe_2O_3 + K_2O + Na_2O + CaO + MgO + MnO + TiO_2)/Al_2O_3] (Cox et al., 1995). Nonclay minerals have a higher ratio of the major cations to Al_2O_3 than clay minerals so the nonclay minerals have a higher ICV. For example, the ICV decreases in the order of pyroxene and amphibole (~10–100),

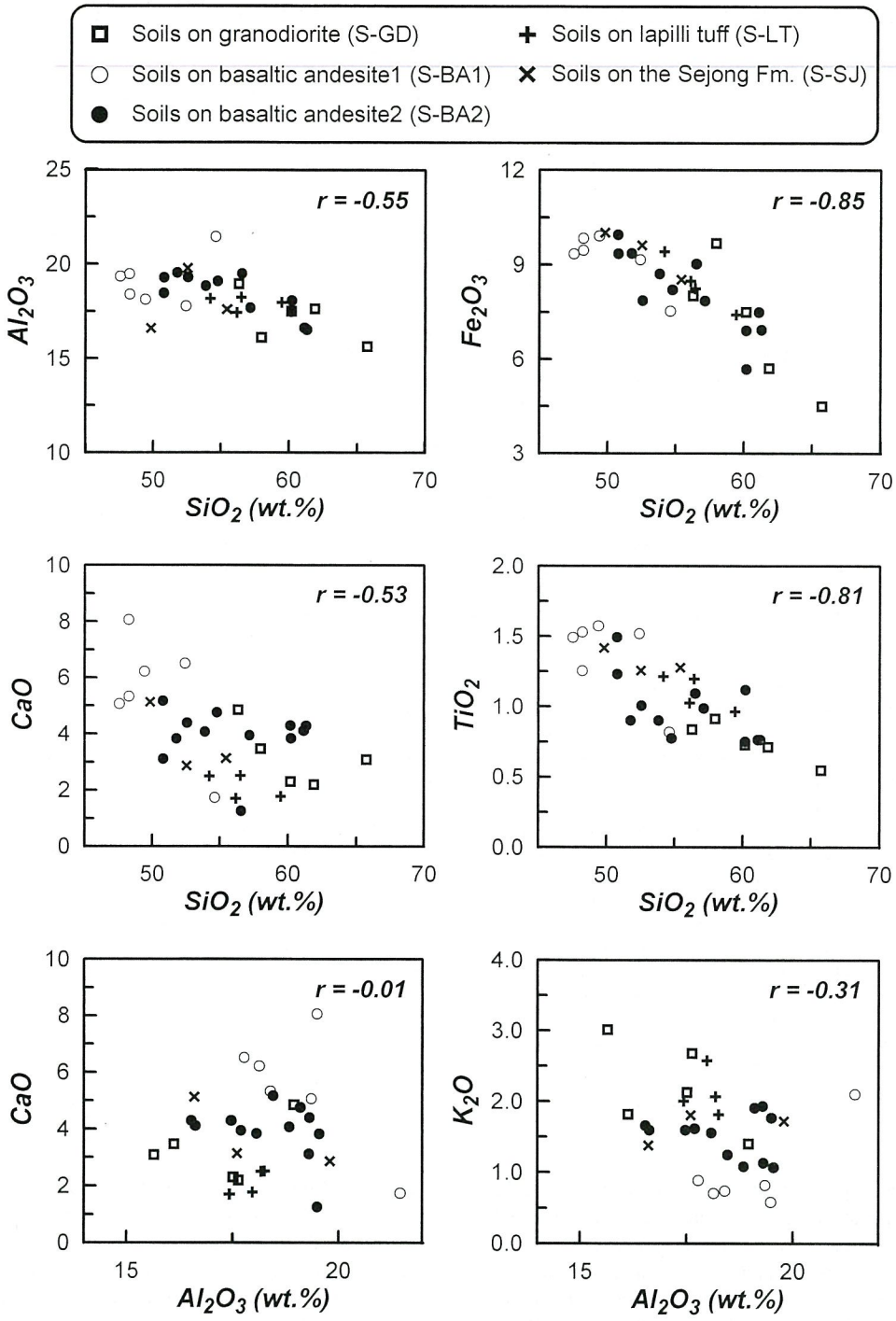

Fig. 3. Bivariate plots of the oxides Al_2O_3, Fe_2O_3, CaO, TiO_2 vs. SiO_2 and CaO, K_2O vs. Al_2O_3 in the fine fractions from Barton Peninsula soils. Note the different symbols for five different soil suites.

biotite (~8), alkali feldspar (~0.8–1), plagioclase (~0.6), muscovite and illlite (~0.3), monmorillonite (0.13–0.3), and kaolinite (~0.03–0.05) (Cox et al., 1995). Thus, immature soils with a high percentage of nonclay silicate minerals will contain ICV values of greater than one. In contrast, more mature soils with mostly clay minerals formed under intense weathering ought to have lower ICV values of less than one (Cox et al., 1995). The ICV values of Barton Peninsula soils range between 1.00 and 1.44 with an average of 1.13 (Table 1). The ICV values of S-GD ranges between 0.9 and 1.3 (av. 1.1), S-BA1 between 0.8 and 1.4 (av. 1.2), S-BA2 between 0.9 and 1.3 (av. 1.1), S-LT between 1.0 and 1.2 (av. 1.1), and S-SJ between 1.0 and 1.4 (av. 1.2), indicating that the Barton Peninsula soils are compositionally immature and dominated by nonclay silicate minerals. All the ICV values of soils except for soils on the Sejong Formation are slightly lower than those of bedrocks. This implies that most of the Barton Peninsula

Table 2. Trace and rare earth element concentrations (ppm) of the Barton Penisula soil samples.

	Soils on granodiorite							Soils on basaltic andesite 1								Soils on basaltic andesite 2			
Sample	237	D1	D3	D14	H1	av.	SD	2311	X1	X14	J6	T4	U3	av.	SD	X4	X5	X8	O1
Rb	46.86	28.34	64.26	65.17	39.71	48.87	15.90	12.76	12.00	15.90	16.58	11.96	42.74	18.66	11.97	40.76	25.96	48.06	41.07
Sr	274.52	439.22	251.56	320.03	325.20	322.11	72.41	237.41	529.22	413.16	389.27	364.25	265.46	366.46	105.88	278.53	336.87	305.59	345.25
Y	13.49	15.69	22.21	19.99	40.95	22.47	10.89	25.33	22.01	26.80	23.67	26.52	11.22	22.59	5.86	19.79	34.78	36.49	18.04
Zr	46.97	29.25	69.99	181.55	55.51	76.65	60.46	99.64	110.02	173.09	72.93	124.32	83.29	110.55	35.72	171.72	166.77	194.13	120.63
Hf	1.32	1.05	2.42	1.76	1.81	1.67	0.52	1.06	3.08	2.73	2.25	4.27	2.56	2.66	1.05	4.80	5.13	5.27	3.92
Nb	2.77	2.76	3.63	3.75	3.79	3.34	0.53	4.12	3.55	4.81	5.40	4.86	2.70	4.24	0.99	3.26	4.72	4.36	3.63
Th	6.23	4.28	6.45	8.79	5.75	6.30	1.63	2.11	1.29	2.14	2.68	1.84	4.01	2.35	0.93	3.63	3.78	4.19	3.97
U	1.51	1.28	6.74	2.12	2.81	2.89	2.23	0.77	0.46	0.65	0.87	0.62	1.07	0.74	0.21	1.35	1.27	1.28	1.13
Cs	2.10	1.91	3.48	2.31	4.04	2.77	0.94	0.97	0.88	1.15	1.95	0.94	2.98	1.48	0.83	2.96	2.89	5.27	0.99
Ba	370.10	296.43	366.98	468.07	293.73	359.06	71.17	101.26	111.05	154.59	173.56	131.51	316.71	164.78	79.11	286.82	224.06	418.77	468.07
La	18.56	18.37	21.76	23.14	24.03	21.17	2.60	11.11	9.50	14.67	15.01	12.46	13.96	12.79	2.17	18.66	31.85	39.48	16.59
Ce	41.39	38.14	52.60	50.90	56.79	47.97	7.87	27.26	23.17	35.15	35.85	30.37	30.18	30.33	4.78	46.85	63.24	71.19	37.69
Pr	5.42	5.29	6.75	6.68	8.15	6.46	1.17	3.85	3.50	5.04	5.11	4.37	3.95	4.30	0.66	5.95	10.45	12.21	5.34
Nd	27.49	26.62	34.94	32.71	41.11	32.57	5.91	20.09	18.05	25.88	26.54	22.58	19.97	22.19	3.44	31.22	50.01	57.65	26.91
Sm	4.62	4.95	6.26	5.64	8.93	6.08	1.71	4.48	4.33	5.43	5.56	4.91	3.44	4.69	0.79	5.79	10.05	11.50	5.30
Eu	1.11	1.42	1.55	1.24	1.90	1.44	0.30	1.58	1.67	1.84	1.83	1.75	1.18	1.64	0.25	1.70	3.06	3.49	1.53
Gd	4.32	5.07	6.66	5.83	10.13	6.40	2.26	5.41	5.22	6.58	6.46	6.13	3.44	5.54	1.17	6.30	10.96	12.32	5.55
Tb	0.55	0.66	0.90	0.76	1.50	0.88	0.37	0.85	0.81	0.97	0.94	0.95	0.44	0.83	0.20	0.84	1.52	1.65	0.76
Dy	2.76	3.45	4.79	4.13	8.56	4.74	2.27	5.04	4.72	5.68	5.22	5.63	2.33	4.77	1.25	4.39	7.82	8.32	4.07
Ho	0.52	0.68	0.94	0.82	1.75	0.94	0.48	1.04	0.99	1.16	1.06	1.16	0.47	0.98	0.26	0.88	1.53	1.58	0.81
Er	1.52	1.97	2.79	2.44	5.19	2.78	1.43	3.04	2.86	3.42	3.02	3.42	1.42	2.86	0.74	2.56	4.30	4.37	2.32
Tm	0.21	0.25	0.36	0.33	0.72	0.37	0.20	0.45	0.37	0.44	0.39	0.44	0.17	0.38	0.11	0.33	0.54	0.54	0.29
Yb	1.41	1.75	2.58	2.30	4.85	2.58	1.35	2.80	2.58	3.09	2.65	3.13	1.34	2.60	0.66	2.35	3.72	3.69	2.04
Lu	0.20	0.25	0.37	0.34	0.73	0.38	0.21	0.43	0.39	0.44	0.39	0.45	0.19	0.38	0.10	0.35	0.53	0.52	0.29
Ni	4.36	11.08	11.69	4.82	12.73	8.93	4.01	18.68	15.65	21.73	17.12	18.46	9.80	16.91	4.02	5.72	14.11	13.85	12.66
Co	8.29	19.09	22.64	10.65	25.58	17.25	7.51	30.22	30.48	28.70	26.09	28.86	11.12	25.91	7.41	23.64	24.68	24.62	28.37
Cu	71.42	148.40	271.27	65.29	109.68	133.21	84.08	110.11	266.47	108.28	141.74	95.32	82.73	134.11	67.77	173.92	123.38	152.81	128.36
Zn	73.00	89.12	180.10	66.81	151.66	112.14	50.74	78.24	80.11	86.55	89.28	86.44	48.27	78.15	15.23	96.23	90.02	103.78	86.96
V	144.99	206.62	148.96	85.32	156.09	148.39	43.13	153.60	250.16	227.74	229.17	222.30	222.32	217.55	32.98	278.11	205.70	209.29	85.32
Cr	14.44	16.34	20.15	6.43	16.45	14.76	5.10	26.62	24.38	37.64	33.87	33.96	26.27	30.46	5.38	6.43	26.98	23.02	14.23
Sc	13.01	19.96	16.31	9.93	18.03	15.45	4.00	14.57	29.09	24.24	27.13	24.82	20.07	23.32	5.26	24.89	26.10	28.20	21.24
Be	1.10	1.77	2.33	1.94	2.56	1.94	0.56	1.20	1.96	2.17	1.76	1.94	1.19	1.70	0.41	2.59	3.11	2.97	2.18
Ga	26.18	27.42	30.08	26.26	26.15	27.22	1.69	21.35	28.23	25.60	25.71	23.99	32.63	26.25	3.86	29.82	29.15	34.15	31.46
Mo	1.31	1.56	1.86	1.73	2.88	1.87	0.60	1.83	0.44	0.67	0.82	1.02	4.17	1.49	1.39	1.20	0.72	1.40	2.12
Cd	0.11	0.11	0.47	0.09	0.55	0.27	0.23	0.23	0.14	0.15	0.12	0.14	<0.06	0.15	0.04	0.14	0.18	0.26	0.10
ΣREE	110.1	108.9	143.3	137.2	174.3	134.76	27.04	87.4	78.2	109.8	110.0	97.8	82.5	94.28	13.76	128.2	199.6	228.5	109.5
Eu/Eu*	0.76	0.87	0.74	0.66	0.61	0.73	0.10	0.99	1.08	0.94	0.94	0.98	1.05	1.00	0.06	0.87	0.90	0.90	0.86
Ce/Ce*	0.96	0.91	1.00	0.97	0.95	0.96	0.04	0.96	0.93	0.95	0.95	0.95	0.95	0.95	0.01	1.02	0.83	0.79	0.94
(La/Sm)n	2.48	2.29	2.15	2.53	1.66	2.22	0.35	1.53	1.35	1.67	1.67	1.56	2.51	1.71	0.40	1.99	1.96	2.12	1.93
(Gd/Yb)n	2.44	2.31	2.06	2.02	1.66	2.10	0.30	1.54	1.62	1.69	1.94	1.56	2.05	1.73	0.21	2.14	2.35	2.66	2.17
(La/Yb)n	8.81	7.02	5.64	6.74	3.31	6.30	2.02	2.65	2.47	3.17	3.79	2.66	6.97	3.62	1.71	5.32	5.72	7.15	5.44

soils are formed by physical disintegration of bedrocks and that components of chemical weathering product such as clay minerals are very minor, suggesting that the chemical weathering has not occurred significantly. This interpretation is in agreement with the conclusion of Jeong and Yoon (2001) who interpreted that clay mineral formation by chemical weathering on the Barton Peninsula seems insignificant. Thus, most of the fine fractions of the Barton Peninsula soils may have been produced by physical weathering, freeze-and-thaw process in particular. Fine fraction formation by glacial comminution is not considered here due to the presence of the stagnant ice cap cover.

6.2. Changes in Major Elements

Al is an element with low solubility in common soil solutions with normal pH values and therefore is a candidate for the immobile element (Brimhall and Dietrich, 1987; Young and Nesbitt, 1998; Birkeland, 1999). TiO_2 is also considered a fairly immobile constituent. However, it is susceptible to loss in extremely alkaline or acidic conditions and if present in volcanic glass rather than a weather-resistant mineral such as rutile or ilmenite. Hamdan and Burnham (1996) and Girty et al. (2003) rank Ti as being more mobile than Al during pedogenesis of granitic rock. Volcanic rocks dominate the bedrocks in the Barton Peninsula. Hence, TiO_2 was not considered to be a viable candidate for the immobile element. By assuming constant Al_2O_3 content, we can estimate the changes (enrichment factor, EF) that have occurred on weathering using the following equation:

$$EF = (E/Al_{soil})/(E/Al_{bedrock}) \quad (1)$$

in which E/Al_{soil} and $E/Al_{bedrock}$ are the concentrations of an element E and of Al in the soil and in the bedrock, respectively.

Table 2. (Continued).

	Soils on basaltic andesite 2										Soils on lapilli tuff						Soils on the Sejong Fm.				
Sample	O12	261	262	263	264	233	231	B11	av.	SD	265	266	X9	X10	av.	SD	M3	P4	261	av.	SD
Rb	32.85	23.79	21.77	23.45	33.29	35.79	34.40	33.39	32.88	8.06	53.01	46.52	62.06	43.45	51.26	8.23	41.29	41.96	32.05	38.43	5.54
Sr	493.64	367.49	342.85	414.66	379.29	369.93	325.96	434.68	366.23	59.00	225.95	251.45	294.66	329.96	275.51	46.07	297.97	285.86	277.07	286.96	10.49
Y	20.94	16.92	17.22	19.89	22.41	15.58	14.69	13.26	20.83	7.40	25.14	22.27	27.18	27.36	25.49	2.37	21.75	28.37	27.88	26.00	3.69
Zr	194.40	40.18	47.01	47.33	49.68	53.30	50.71	42.82	98.22	65.60	107.43	154.82	225.85	209.26	174.34	53.95	181.55	163.57	144.60	163.24	18.48
Hf	5.64	1.14	1.19	1.38	1.57	1.94	1.88	1.51	2.95	1.83	3.00	5.01	6.43	5.84	5.07	1.50	4.60	4.53	4.07	4.40	0.29
Nb	4.90	3.26	2.94	3.00	0.42	3.45	2.90	2.88	3.31	1.16	3.33	3.72	4.03	4.47	3.89	0.48	4.22	5.24	3.08	4.18	1.08
Th	5.46	3.89	3.96	3.06	3.99	4.46	4.83	4.43	4.14	0.61	4.65	5.18	5.86	4.65	5.09	0.57	3.50	3.78	2.76	3.35	0.53
U	1.82	0.88	1.34	0.98	1.14	1.43	1.32	1.38	1.28	0.24	1.40	1.51	1.78	1.50	1.55	0.16	1.06	1.33	0.98	1.12	0.19
Cs	0.83	2.10	2.06	3.05	2.20	1.33	1.19	1.43	2.19	1.24	3.28	1.28	3.85	2.08	2.62	1.16	4.26	3.25	3.38	3.63	0.55
Ba	369.03	274.19	260.91	244.75	356.14	304.29	280.69	315.40	316.93	73.02	346.86	398.52	463.26	333.98	385.65	58.77	301.39	343.71	212.35	285.82	67.05
La	24.46	17.09	16.88	16.24	28.36	16.86	16.64	16.31	21.62	7.74	26.22	19.69	32.93	26.99	26.46	5.42	17.02	32.67	18.05	22.58	8.75
Ce	54.96	38.76	38.39	37.53	65.18	37.30	36.83	35.84	46.98	13.08	59.27	46.24	75.58	64.41	61.37	12.17	40.26	65.41	40.36	48.68	14.49
Pr	7.38	5.24	5.19	5.13	8.48	4.91	4.83	4.89	6.67	2.47	7.94	6.23	10.27	8.67	8.28	1.68	5.81	10.26	5.85	7.31	2.56
Nd	36.51	27.07	26.78	26.53	43.66	25.00	24.63	24.39	33.36	11.22	40.47	32.05	51.86	44.45	42.21	8.25	29.12	49.53	29.66	36.10	11.63
Sm	6.55	5.17	5.03	5.19	7.94	4.43	4.33	4.36	6.30	2.34	7.38	6.08	9.38	8.26	7.77	1.39	5.96	9.65	6.15	7.25	2.08
Eu	2.01	1.42	1.38	1.48	2.29	1.30	1.19	1.32	1.85	0.74	2.00	1.58	2.53	2.38	2.12	0.43	1.87	2.72	1.94	2.17	0.47
Gd	6.85	5.22	5.06	5.45	7.73	4.44	4.16	4.38	6.54	2.62	7.48	6.13	9.81	8.72	8.03	1.59	6.39	9.98	6.80	7.72	1.96
Tb	0.92	0.68	0.66	0.74	0.97	0.60	0.53	0.57	0.87	0.36	0.96	0.83	1.24	1.15	1.05	0.19	0.90	1.27	0.97	1.05	0.20
Dy	4.80	3.50	3.52	3.99	4.96	3.09	2.91	2.98	4.53	1.79	4.98	4.38	6.24	6.00	5.40	0.87	4.98	6.36	5.45	5.60	0.70
Ho	0.93	0.66	0.67	0.77	0.89	0.61	0.56	0.58	0.87	0.34	0.94	0.87	1.19	1.19	1.04	0.17	1.00	1.21	1.07	1.09	0.11
Er	2.70	1.87	1.90	2.23	2.46	1.80	1.68	1.71	2.49	0.93	2.70	2.57	3.40	3.44	3.03	0.46	2.92	3.37	3.10	3.13	0.23
Tm	0.35	0.25	0.25	0.30	0.31	0.25	0.23	0.20	0.32	0.11	0.36	0.36	0.43	0.45	0.40	0.05	0.39	0.42	0.42	0.41	0.02
Yb	2.48	1.55	1.61	1.91	2.00	1.67	1.57	1.58	2.18	0.78	2.39	2.40	3.02	3.09	2.73	0.38	2.73	2.84	2.80	2.79	0.05
Lu	0.35	0.22	0.23	0.27	0.27	0.24	0.23	0.21	0.31	0.11	0.35	0.36	0.44	0.46	0.40	0.06	0.40	0.41	0.40	0.40	0.00
Ni	10.93	21.87	13.66	15.04	7.54	6.90	7.09	8.90	11.52	4.62	8.11	7.85	5.28	10.23	7.87	2.03	9.32	8.31	9.78	9.14	0.75
Co	20.29	30.95	20.60	24.18	18.08	12.53	15.55	12.66	21.34	5.84	22.30	20.97	18.81	23.85	21.48	2.13	21.64	18.78	23.36	21.26	2.31
Cu	165.31	177.50	137.40	184.51	119.70	67.36	66.66	94.76	132.64	40.70	137.20	91.68	164.40	115.76	127.26	30.97	165.92	92.60	113.70	124.07	37.75
Zn	66.58	98.25	88.19	88.19	93.13	65.43	63.83	71.96	84.38	13.84	86.62	89.03	91.36	100.62	91.91	6.12	99.49	93.36	88.58	93.81	5.47
V	187.10	184.70	168.19	183.86	56.98	148.57	143.36	169.92	168.43	57.44	171.84	178.70	175.66	205.05	182.81	15.09	254.89	174.55	185.25	204.90	43.62
Cr	18.69	39.03	24.80	33.58	12.29	14.12	13.88	17.01	20.34	9.47	11.30	16.45	6.27	16.07	12.52	4.78	20.68	12.77	14.36	15.94	4.19
Sc	23.14	18.85	16.82	18.41	17.27	11.73	11.32	16.03	19.50	5.37	16.25	18.03	19.60	22.09	18.99	2.48	29.06	21.74	16.79	22.53	6.18
Be	2.37	1.17	1.31	1.16	1.69	1.09	1.10	1.76	1.88	0.75	1.62	1.43	2.93	2.40	2.09	0.70	1.95	2.79	1.32	2.02	0.74
Ga	29.66	24.70	23.88	24.52	26.66	22.82	22.22	25.42	27.04	3.75	26.51	25.51	35.60	31.77	29.85	4.72	29.61	31.68	23.71	28.33	4.13
Mo	0.49	1.27	1.49	0.72	<0.05	1.67	1.69	2.12	1.35	0.55	1.67	1.06	1.25	0.46	1.11	0.50	1.58	1.86	2.21	1.89	0.32
Cd	0.12	0.18	0.12	0.21	0.09	0.10	0.10	0.08	0.14	0.05	0.23	0.22	0.16	0.36	0.24	0.08	0.13	0.17	0.19	0.16	0.03
TREE	151.2	108.7	107.5	107.8	175.5	102.5	100.3	99.3	134.88	43.94	163.4	129.8	208.3	179.7	170.3	32.77	119.7	196.1	123.0	125.9	43.17
Eu/Eu*	0.92	0.84	0.84	0.85	0.90	0.90	0.86	0.93	0.88	0.03	0.83	0.79	0.81	0.86	0.82	0.03	0.93	0.85	0.92	0.89	0.04
Ce/Ce*	0.97	0.95	0.95	0.95	0.97	0.96	0.96	0.95	0.92	0.06	0.96	0.97	0.98	0.96	0.97	0.01	0.95	0.86	0.92	0.90	0.05
(La/Sm)n	2.30	2.04	2.07	1.93	2.20	2.35	2.37	2.31	2.13	0.17	2.19	2.00	2.17	2.02	2.09	0.10	1.76	2.09	1.81	1.95	0.18
(Gd/Yb)n	2.20	2.69	2.50	2.28	3.08	2.12	2.12	2.21	2.38	0.30	2.49	2.04	2.59	2.25	2.34	0.25	1.86	2.80	1.94	2.07	0.52
(La/Yb)n	6.58	7.39	7.00	5.69	9.49	6.77	7.11	6.91	6.71	1.14	7.32	5.49	7.30	5.84	6.49	0.96	4.16	7.68	4.32	5.29	1.99

Generally, compared to bedrocks (Table 3) enrichment or depletion of major elements in Barton Peninsula soils are slight, except for Ca and Mn depletion and P enrichment in some soils (Fig. 5). For these elements the changes are less than a factor of 2. Phosphorous enrichment in S-BA1 and S-SJ soils appears to have been caused by the influence of excreta of skua gulls and penguins. This interpretation is supported by high correlation coefficient ($r = 0.78$) between phosphorous enrichment factor (EFp) and TOC in soils. Especially, soils with high TOC content were collected close to the nesting sites of skua gulls and to the coastal areas where a penguin rookery is situated. Its characteristic is something like ornithogenic soils as described by Tedrow and Ugolini (1966). For the King George Island region Myrcha and Tatur (1991) postulated that iron was entirely leached from the soil by strong action of guano solutions. However, relatively phosphate-enriched soils, S-BA1 and S-SJ, do not show any Fe depletion phenomenon (Fig. 5), indicating that probably these soils were not affected much from guano solutions. Slight K- and Ti-enrichment is also noted in S-BA1. K_2O content in BA1 is quite low (Table 3) and thus mixing of soil materials from K_2O -rich bedrock, most probably neighboring granodiorite, might have caused the K-enrichment in S-BA1. The converse may be applicable to slight K-depletion in S-GD. Mixing of pumice shards that are abundantly observed in S-BA1 may have influenced the Ti-enrichment in this soil suite.

In the Barton Peninsula lichens growing on rock and rock debris surfaces or on soils seem to be an important agent bringing about chemical weathering (e.g., Schatz, 1963; Jackson and Keller, 1970). Among the major elements Ca is the one most depleted in the S-GD, S-BA1 and S-BA2 soils compared to the bedrocks (Fig. 5). Such Ca depletion is more prominent in soils developed on basaltic andesite (S-BA1 and S-BA2) than those in other bedrocks. Depletion of Ca associated with

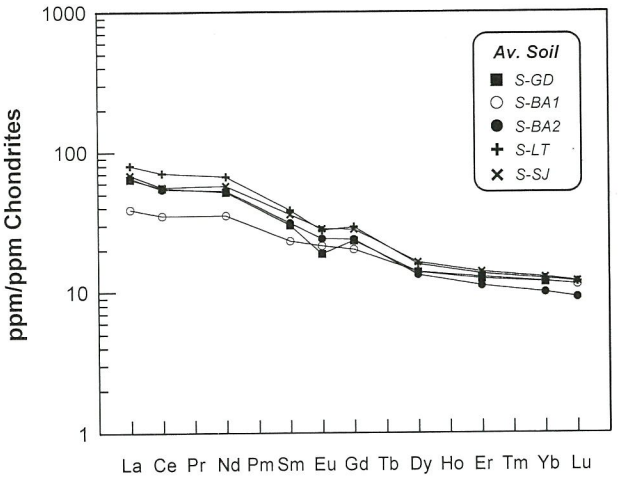

Fig. 4. Chondrite-normalized REE distribution patterns of Barton Peninsula soil suites. All but the S-BA1 show a similar general distribution pattern. The S-BA1 displays a lesser fractionated pattern and has no europium anomaly.

slight depletion of Na and Sr (Table 2) in these soils is controlled by alteration of plagioclase. Alternatively and more probably, soils and rock debris on basaltic andesite and granodiorite are much covered by lichens, suggesting that Ca depletion is largely controlled by chelating agent excreted by lichens as demonstrated in the weathering of Hawaii basalt (Jackson and Keller, 1970). Little change of Fe and Mn indicates that the weathering occurred under oxidizing conditions. Only samples collected in topographically low areas show slight depletion of both Fe and Mn, due to the sluggish water movement and poor drainage. Such little change in Fe indicates that microbial activity in the soils was minimal in the Barton Peninsula (e.g., Wierzchos et al., 2003). A recent study suggests that lichens are not active under snow cover (Pannewitz et al., 2003) and thus implying that their contribution to biologic weathering during the glacial times was minimal and that chemical weathering due to lichens began after deglaciation and is active during the summer period.

6.3. Degree of Chemical Weathering

Nesbitt and Young (1982, 1984) suggested a method for quantifying the degree of chemical weathering to which rocks have been subjected. This measure, called the chemical index of alteration (CIA), is based on the formula

$$CIA = [Al_2O_3/(Al_2O_3 + CaO^* + Na_2O + K_2O)] \times 100 \quad (2)$$

where values are expressed as molar proportions and CaO* represents CaO in silicate mineral only. The CIA gives a measure of the ratio of original, primary minerals and secondary products such as clay minerals. Usually, CIA ranges from ~50, for fresh rocks, to 100 for completely weathered rocks, composed entirely of secondary minerals such as kaolinite and gibbsite. CIA values for various estimates of "average" shales fall between 70 and 75. For calculation of CIA values, one needs to consider P enrichment in the soil samples. Phosphorous contents in the studied soils are not related to the amount of apatite, but to the contribution from ejecta of skua gulls and penguins. This is evidenced by a good correlation between TOC and P_2O_5 (r = 0.76). Such contribution from biologic factors may confuse the interpretation of weathering intensity of the bedrocks. To correct this influence, samples with EFp values larger than 1.0 are assumed to have the maximum P content of the bedrock. Also, soils developed on the Sejong Formation are enriched in Ca by nearby penguin rookeries. Here again Ca content of the Ca-enriched soils is assumed to have the maximum content as that of the Sejong Formation.

CIA values of Barton Peninsula soils ranges between 49.6 and 77.3 with an average of 59.2 (Table 1). S-BA ranges between 49.6 and 77.3 (average 58.2; S-BA1 = 57.5, S-BA2 = 58.6) and S-GD between 51.7 and 63.7 (average 57.5). Average CIA values in the two soil suites are equal at 5% level of significance. The highest CIA value (77.3) is observed in sample U3 developed on BA1. This soil sample is characterized by enriched K_2O and Al_2O_3 and depleted CaO and Na_2O contents compared with other soil samples (Table 1). Considering its location, this may not be due to high degree of chemical weathering, but due to the nature of bedrock having undergone phyllic to argillic alteration by paleohydrothermal activity (e.g., Park, 1990; Hur et al., 2001).

The Al_2O_3-(CaO* + Na_2O)-K_2O diagram of Barton Peninsula soils are shown in Figure 6. Also shown are average bedrock compositions of granodiorite, basaltic andesite, lapilli tuff, and the Sejong Formation. Generally, plots of soils in soil profiles trend almost parallel to the A-CN boundary, and the intersection point of lines through data and the feldspar join represents the source composition. In Figure 6 the probable weathering trends of basaltic andesite and granodiorite are represented by broken arrows. All soils plot in the space between the weathering trends of basaltic andesite and granodiorite. Soils on basaltic andesites (S-BA1 and S-BA2) plot on the general weathering trends of respective bedrocks. However, plots of soil samples on the granodiorite do not show any trend. Half of them follow the weathering trend and the other half are shifted towards the A-CN tie line, most probably by K_2O depletion. Compared to CaO and Na_2O, K_2O tends to be fixed in the clay minerals during weathering. Thus, K_2O depletion in the latter soils on granodiorite may not be caused by chemical weathering. The most plausible explanation is that soils that do not follow the granodiorite weathering trend might have been mixed with other soil materials having less K_2O content (see below).

As shown in Figure 6 soil samples have generally higher CIA values than bedrocks, indicating that bedrocks have undergone some degree of chemical weathering. Accordingly, although not apparent in the ICV values, Barton Peninsula soils would contain some secondary minerals formed during chemical weathering. Jeong and Yoon (2001) reported that the soil clay minerals are chlorite, illite, smectite, and kaolinite, and comprise on average 20–30% of soil samples <200 mesh. They showed that distribution of illite and kaolinite is highly localized, mostly on the altered bedrocks, whereas smectite is uniformly distributed. Smectite is associated with the widespread pumice shards in the soils, especially in the early-deglaciated western margin of the peninsula, which is indicative of their origin from eolian pumice shards rather than as an in situ weathering product (Jeong and Yoon, 2001). A consid-

Table 3. Average major, trace elements and REE data for the source rocks for soils on the Barton Peninsula.

Sample	Granodiorite (n = 18)[a]	Basaltic andesite1 (n = 23)[b]	Basaltic andesite2 (n = 14)[b]	Lapilli tuff (n = 3)[c]	Sejong Fm. (n = 2)[c]	Pumice shards (n = 9)[d]	Pampean loess (n = 8)[e]
SiO_2	63.22	51.48	54.90	58.46	51.30	53.11	
TiO_2	0.50	0.72	0.81	0.89	1.09	2.28	
Al_2O_3	15.69	19.12	17.16	16.92	20.30	15.49	15.24
Fe_2O_3	4.79	8.40	7.96	7.60	9.75	9.46	
MnO	0.11	0.16	0.14	0.14	0.29	0.20	
MgO	2.12	4.52	3.58	2.56	2.87	3.84	
CaO	4.36	9.37	7.27	2.75	3.11	8.30	5.42
Na_2O	3.91	3.08	3.21	3.06	3.30	3.86	2.36
K_2O	3.15	0.50	1.43	1.93	1.92	0.64	2.31
P_2O_5	0.15	0.16	0.27	0.33	0.22	0.46	0.16
LOI	1.53	2.52	3.18	4.27	5.62		
total	99.52	100.02	99.91	94.63	94.16	97.64	
Be				1.63	1.13		
Sc	14.50	24.81	25.39	16.54	21.63	30.33	
V		215.66	193.59	177.46	180.37	278.67	
Cr		14.52	11.93	8.36	12.65	49.67	
Co	19.73	26.05	23.02	17.32	27.96	31.56	
Ni		14.43	17.95	5.66	8.02	62.78	
Cu	168.21	108.57	134.31	81.51	62.85	50.89	
Zn	90.49	69.66	83.31	93.47	140.80	75.67	
Ga		18.26	20.27	25.71	26.17		
Rb	80.55	7.46	21.80	44.01	48.76	12.11	80.88
Sr	383.71	608.86	622.44	346.33	335.90	366.00	306.25
Y	24.06	12.27	21.13	22.23	20.10	38.11	22.98
Zr	121.2[f]	50.70	144.50	134.40	90.42	164.22	
Nb	10.98	1.38	3.34	14.27	3.39	5.89	9.98
Mo		0.65	1.52	1.25	0.66		
Cd				0.19	0.26		
Sn		1.13	1.22				
Cs		0.97	0.69	1.26	4.58		4.93
Ba	382.29	133.08	367.22	387.34	276.08	94.89	575.25
La	18.22	8.39	18.51	21.26	12.94	11.64	24.01
Ce	40.69	19.21	43.70	48.48	31.65	30.22	49.21
Pr		2.64	5.52	6.67	4.15	4.28	6.51
Nd	20.71	12.37	25.40	34.12	22.01	20.64	23.30
Sm	4.25	3.03	5.72	6.42	4.52	5.03	4.76
Eu	1.08	1.05	1.45	1.58	1.52	1.85	1.11
Gd	4.74	2.81	4.70	6.49	4.94	6.39	4.17
Tb		0.43	0.69	0.84	0.70		0.63
Dy	3.79	2.54	4.22	4.44	3.98	6.74	3.67
Ho		0.50	0.86	0.85	0.80	1.28	0.75
Er	2.09	1.42	2.31	2.48	2.31	3.60	2.07
Tm				0.33	0.31		0.33
Yb	1.94	1.27	1.94	2.22	2.05	3.41	2.17
Lu		0.18	0.29	0.32	0.29	0.52	0.32
Hf		1.57	3.73	3.71	2.40		
Ta		0.14	0.31				0.79
W		7.44	0.24				
Pb	14.33	4.69	6.63	8.22	5.89		18.01
Bi				0.55	0.28		
Th	7.47	1.41	3.13	4.75	1.79		8.88
U		0.40	1.06	1.38	0.50		2.03
ΣREE	97.52	55.85	115.31	136.50	92.17	95.61	123.01
Eu/Eu*	0.74	1.11	0.86	0.75	0.99	1.00	0.77
(La/Sm)n	2.65	1.71	2.00	2.04	1.77	1.43	3.12
(Gd/Yb)n	1.94	1.76	1.93	2.33	1.92	1.49	1.53
(La/Yb)n	6.27	4.42	6.38	6.41	4.22	2.28	7.40
Th/Sc	0.51	0.06	0.12	0.29	0.08		

[a] After Lee et al. (2001).
[b] After Yeo et al. (2004).
[c] This study.
[d] After Jwa and Kim (1991).
[e] After Gallet et al. (1998).
[f] After Jin et al. (1991) (n = 5).

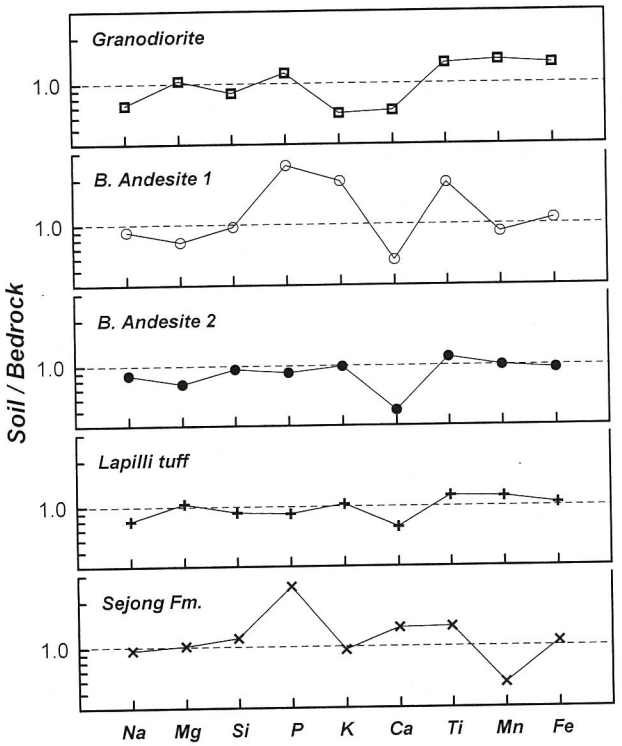

Fig. 5. Spider plots of average Al-normalized major element compositions of each soil suite normalized against each corresponding bedrock. Slight phosphorus enrichment is observed in S-BA1 and S-SJ soils, whereas very slight depletion of Ca is observed in S-BA1 and S-BA2.

erable amount of pumice shards is observed in the Barton Peninsula soils. Jeong and Yoon (2001) explained that clay minerals (smectite) in the soil are mostly derived from these

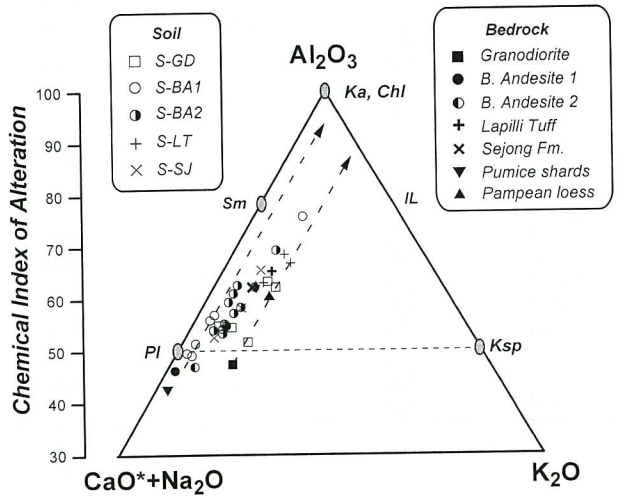

Fig. 6. A (Al_2O_3) − CN (CaO^*+Na_2O) − K (K_2O) plot of Barton Peninsula soil suites and bedrocks. Broken arrows represent the predicted weathering trends of granodiorite and basaltic andesite. All soil samples plot in space defined by these two weathering trends. The diagram indicates that the Barton Peninsula soils have not undergone chemical weathering degree sufficient to smectite.

pumice shards, which were derived from Deception Island located southwest of King George Island. They noted that the presence of both fresh and altered pumice shards in the soils indicates their characteristics derived from the source, and not from in situ weathering in the Barton Peninsula. Contribution of eolian pumice shards might have been occurred after deglaciation in King George Island, ca. 6000 yr BP. The fresh pumice shards have average CIA and ICV values of 42.4 and 1.83, respectively. The higher smectite content in the early-deglaciated region of the Barton Peninsula suggests their deposition mostly after deglaciation and not as the residues after ablation of glaciers and ice sheets.

If this is the case, the high CIA values of soils may not indicate the chemical weathering of the bedrocks in the Barton Peninsula, but represent the results of mixing with eolian pumice shards. The CIA value of average fresh pumice shards is lower than those of bedrocks in the Barton Peninsula (Fig. 6). However, the altered glasses of brown color in the soils of the Barton Peninsula have textures very similar to the palagonite shown in Zhou and Fyfe (1989). Thus, glass in pumice shards might be altered to smectite in the hydrothermal environment around the crater of an active volcano or in the submarine weathering environment and reworked by subsequent eruptions. Both fresh pumice shards formed by new eruptions and reworked fresh and smectite-bearing pumice shards have been deposited in King George Island (Jeong and Yoon, 2001). The higher smectite content in soils on granodiorite and basaltic andesite (Jeong and Yoon, 2001) also support the higher CIA values of these soils than bedrocks. Thus, various CIA values of soils would indicate the varying mixing ratios of eolian smectite-bearing pumice shards. This interpretation is supported by the CIA values of soils less than that of smectite (Fig. 6). Parent-material uniformity of the Barton Peninsula soils was checked by ratios of element oxides that reside in resistant minerals. Common oxide ratios are Y_2O_3/ZrO_2 and ZrO_2/TiO_2 (Marsan et al., 1988; Reheis, 1990). Table 4 shows that Barton Peninsula soils have different oxide ratios from bedrocks. Also, these oxide ratios are different among soil samples. The results indicate nonuniformity of parent materials, attributing to varying degrees of mixing of allogenic components including eolian pumice shards. The result of this study suggests that the CIA value of soils for measure of chemical weathering degree should be used with caution.

6.4. REE Distribution Patterns of Bedrocks

Average REEs of bedrocks of the Barton Peninsula are tabulated in Table 3 and shown in Figure 7. Among bedrocks basaltic andesite 1 (BA1) has the least total REE content of 55.9 ppm and has a least fractionated REE distribution pattern with (La/Sm)n = 1.7, (Gd/Yb)n = 1.8 and (La/Yb)n = 4.4. It shows positive europium anomaly (Eu/Eu* = 1.11). BA2 has total REE concentration of 115.3 ppm and slightly more fractionated REE distribution than BA1 [La/Sm]n = 2.0, (Gd/Yb)n = 1.9 and (La/Yb)n = 6.4]. Granodiorite has total REE concentration of 97.5 ppm with a slightly fractionated REE pattern having (La/Sm)n = 2.7, (Gd/Yb)n = 1.9 and (La/Yb)n = 6.3 and pronounced negative Eu anomaly (Eu/Eu* = 0.74). Compared to other bedrocks lapilli tuff contains slightly higher REE concentrations of 136.5 ppm and shows also slightly fraction-

Table 4. Oxide ratios of bedrocks and soils of the Barton Peninsula.

Sample	Y_2O_3/ZrO_2 (×1000)	ZrO_2/TiO_2 (×1000)
Bedrocks		
granodiorite	186.6	32.7
basaltic andesite1	227.5	4.8
basaltic andesite2	137.5	13.8
lapilli tuff	155.5	20.4
Sejong Fm	209.0	11.2
Soils		
S-GD		
237	270.1	8.7
D1	504.5	4.7
D3	298.3	13.3
D14	103.5	44.7
H1	693.5	8.2
S-BA1		
2311	239.0	8.8
X1	188.1	11.8
X14	145.6	15.4
J6	305.2	6.6
T4	200.6	10.7
U3	126.6	13.8
S-BA2		
X4	108.3	21.2
X5	196.0	15.1
X8	176.7	21.3
O1	140.6	21.0
O12	101.3	23.4
261	395.9	6.0
262	344.4	7.0
263	395.2	6.3
264	424.1	6.8
233	274.9	9.4
2310	272.4	9.0
B11	291.2	7.7
S-LT		
265	220.0	14.1
266	135.2	17.2
X9	113.1	31.6
X10	122.9	23.6
S-SJ		
M3	112.6	19.5
P4	163.1	17.3
2612	181.3	13.8

ated REE pattern with (La/Sm)n = 2.0, (Gd/Yb)n = 2.3 and (La/Yb)n = 6.4. The negative Eu anomaly is similar to that of granodiorite, Eu/Eu* = 0.75, and characteristically lapilli tuff has lightly negative Ce anomaly. The least REE fractionation is also observed in the Sejong Formation, which has REE concentration of 92.2 ppm with (La/Sm)n = 1.8, (Gd/Yb)n = 1.9 and (La/Yb)n = 4.2. The Sejong Formation show no Eu anomaly (Eu/Eu* = 0.99).

6.5. REE Distribution Patterns of Soils

The REEs of studied soils have slightly different distribution patterns from those of respective bedrocks (Fig. 8). Also, all soil samples have total REE contents ~30% higher than respective bedrocks. The REE enrichments in the studied soils compared to bedrocks would indicate some degrees of chemical weathering of bedrocks. Most soil samples show slightly fractionated distribution patterns compared to bedrocks except for S-BA1. The latter displays lesser fractionation than the

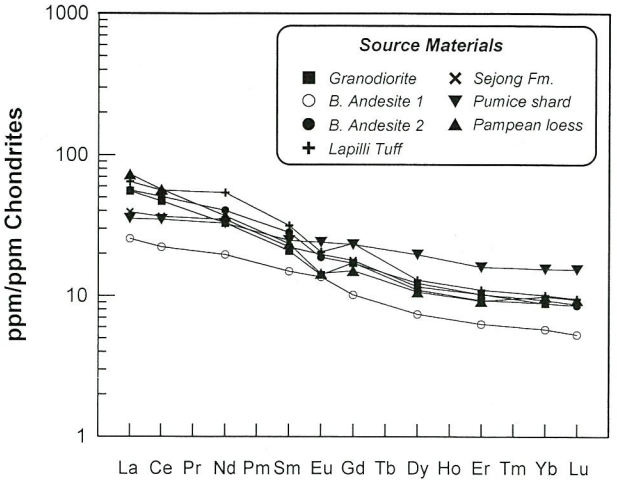

Fig. 7. Chondrite-normalized REE distribution patterns of Barton Peninsula bedrocks showing different REE characteristics in terms of fractionation and Eu anomaly.

bedrock [(La/Yb)n = 3.6 vs. 4.4]. REEs are known to be mobile during weathering, at least within the profile, particularly during the early stage of weathering (Nesbitt, 1979; Condie, 1991). Nesbitt (1979) showed that REE net losses or gains of specific REEs are not observed, that is, they do not leave the system. In this study REE mobility in surface soils is assumed to be negligible based on the low chemical weathering degrees as evidenced by slight changes in major elements compared to bedrocks. Homogeneous REE distribution patterns in each soil suite also suggest that the soil REEs were not affected much during weathering, but rather are controlled by source material characteristics. In the S-GD, S-BA2, and S-LT the REE characteristics are similar but with slight differences to those of bedrocks, whereas slightly lesser fractionation and slightly more fractionation in REEs are observed in the S-BA1 and S-SJ, respectively (Tables 2 and 3). Thus, it is interpreted that mobilization and fractionation of REEs during the chemical weathering was relatively insignificant and that the REE characteristics resulted from mixing of different source components. Considering that REEs are transferred to soils quantitatively from bedrocks during weathering the different REE distribution patterns of the soils compared to corresponding bedrocks indicate that the REE characteristics of each soil suite were not solely inherited from the bedrocks, but may reflect the varying importance of extra materials, such as adjacent parent materials and eolian additions relative to contributions from the respective parent material. This interpretation is supported by the presence of pumice shards in the studied soils (Fig. 2) and by the deviations of soil compositions from the predicted weathering trends of bedrocks (Fig. 6). Considering the presence of altered (smectite-bearing) pumice shards in the studied soils the enrichment of REEs in soils compared to bedrocks may not have been totally due to the in situ chemical weathering, but have been largely controlled by the mixing of altered allogenic materials.

Very slight negative Ce anomalies are observed in some soil samples, although they are not observed in basement rocks except for lapilli tuff (Fig. 8). This observation is interpreted as

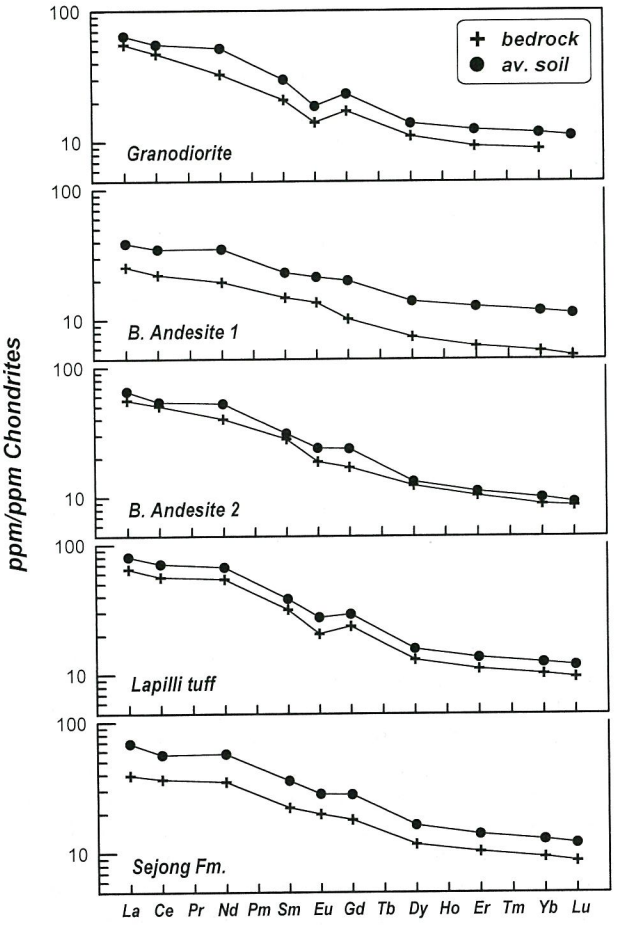

Fig. 8. Comparison of REE distribution patterns between Barton Peninsula soil suites and bedrocks. The REE characteristics between the soil and bedrock are slight different from each other.

the incipient weathering of parent rocks, because the negative Ce anomalies are well developed in weathering profiles of magmatic rocks (Nesbitt, 1979; Duddy, 1980; Lottermoser, 1990; Nesbitt and Wilson, 1992) linked with the REE enrichments. According to the above authors, oxidation of Ce^{3+} to Ce^{4+} during weathering results in its fixation in the most altered part of the weathering profiles. It is well known that decoupling of Ce from the other REEs typically occurs in oxidizing low-temperature environments. The soil samples for this study were collected from the surface soils, and so one would not expect to have negative Ce anomalies in this part of the soil profiles. If the negative Ce anomaly in soils is caused by the descending REE-bearing aqueous fluids through the soil profile, such negative Ce anomaly in the studied soils needs to be noted. Three possible mechanisms can be inferred to explain its occurrence. First, the most altered active layers have been eroded out and the collected surface soils may represent the former soil horizons subjacent to the eroded part. If erosion had occurred, the most likely mechanism is glacier movement. However, the present Barton Peninsula is covered by stable ice cap and there is no record of glacier advance since the last deglaciation. Second, bioturbation may have caused mixing between the surface soils and the soils located underneath the topsoil. However, this interpretation is less likely due to the near absence of burrowing organisms and lack of vegetation in the maritime Antarctic region. Lastly and most probably, the surface soils were mixed with the soils beneath it as a result of cryoturbation such as frost heave, the same mechanism responsible for the formation of patterned ground. However, it needs further study to confirm this possibility.

6.6. Mixing Results

Bedrocks in the Barton Peninsula soils are granodiorite, basaltic andesite, lapilli tuff, and the Sejong Formation. In addition to these bedrocks, eolian input is also considered as a potential contributor. As discussed above, pumice shards from Deception Island constitute an important eolian addition. Pumice shards have average total REE content of 95.6 ppm with little fractionated REE distribution [(La/Yb)n = 2.3] and no europium anomaly (Table 3). As an additional eolian source it is well known from ice core studies in Antarctica that atmospheric transport of dust has been continuous and that dusts have been contributed from Patagonia region of South America (Grousset et al., 1992; Basile et al., 1997). Transport of dust to Antarctica is likely to be achieved by deflation from loess sites in Patagonia by westerly winds, followed by entrainment in the circum polar vortex, the cyclonic circulation cell centered on Antarctica (Basile et al., 1997; Iriondo, 2000). As a representative of the Patagonian dust source, we choose Pampean loess deposits in Argentina (Gallet et al., 1998). The Pampean loess has CIA and ICV values of 60.3 and 1.13, respectively (Table 3), indicating that the Patagonian dust source has signatures of a weak degree of chemical weathering (Fig. 6) and immature, nonclay silicate mineral composition. It has average total REE content of 123.0 ppm and shows a fractionated REE distribution pattern having fractionated LREEs [(La/Sm)n = 3.1], almost flat HREEs [(Gd/Yb)n = 1.5] and negative europium anomaly (Eu/Eu*) of 0.75 (Table 3). Considering the grain size of eolian dusts in the atmosphere transport, the dusts from the Patagonian origin might have contributed to the fine fraction of the studied soils.

As shown in Figure 7 all the above-mentioned sources have characteristically different REE distribution patterns, thus enabling us to quantify the contribution of different sources to the Barton Peninsula soils. With recognition of the above-mentioned source contributors, we attempted to quantitatively model the relative proportions of these contributors in each soil suite using the REE data. A seven-component mixing calculation has been performed by assuming conservation of mass balance amongst the relatively immobile REEs. Considering the geology and topography of the study area, each soil suite can be assumed to have maximum of four different sources out of seven end members. For example, soils on lapilli tuff (S-LT) have contributions from sources of lapilli tuff, basaltic andesite 2, pumice shards and Pampean loess. Modeling was carried out on the average compositions of each suite, relative to chondrite.

Mixing parameters and results are listed in Table 5 and depicted in Figure 9. Mixing calculations show that as expected, bedrocks were the major influence on the REE compositions of fine fractions of the overlying soils, with proportions ranging from 45% for S-BA1 to 75% for S-LT. The modeled mixes also show that significant amounts of externally derived

Table 5. Mixing parameters and results.

	Mixing end members							Soil					Mix results[a]				
Element	GD	BA1	BA2	LT	SJ	PS	PL	S-GD	S-BA1	S-BA2	S-LT	S-SJ	M-GD	M-BA1	M-BA2	M-LT	M-SJ
La	55.39	25.50	56.26	64.63	39.35	35.39	72.99	64.36	38.86	65.70	80.42	68.64	52.65	35.70	57.64	63.17	47.79
Ce	47.04	22.21	50.52	56.04	36.59	34.93	56.89	55.45	35.07	54.31	70.95	56.27	44.97	32.01	50.35	54.52	43.03
Nd	32.87	19.63	40.32	54.16	34.94	32.77	36.98	51.70	35.21	52.96	66.99	57.31	32.60	27.29	38.69	49.99	38.31
Sm	20.94	14.93	28.18	31.65	22.24	24.77	23.43	29.94	23.11	31.05	38.29	35.74	21.46	20.01	26.57	30.14	24.73
Eu	14.07	13.64	18.83	20.53	19.75	24.04	14.40	18.74	21.32	23.99	27.58	28.24	15.58	17.90	17.95	19.92	19.33
Gd	17.19	10.18	17.03	23.50	17.90	23.14	15.12	23.20	20.08	23.68	29.11	27.98	17.53	16.21	17.06	22.00	18.10
Dy	11.05	7.41	12.30	12.95	11.61	19.64	10.69	13.81	13.91	13.20	15.74	16.31	12.12	12.81	12.30	13.00	11.87
Er	9.28	6.31	10.27	11.00	10.25	16.02	9.19	12.37	12.73	11.07	13.46	13.92	10.14	10.63	10.30	11.00	10.28
Yb	8.84	5.77	8.82	10.08	9.33	15.51	9.87	11.72	11.81	9.91	12.39	12.69	9.79	10.23	9.31	10.21	9.31
$(La/Sm)_N$	2.65	1.71	2.00	2.04	1.77	1.43	3.12	2.15	1.68	2.12	2.10	1.92	2.45	1.78	2.17	2.10	1.93
$(Gd/Yb)_N$	1.94	1.76	1.93	2.33	1.92	1.49	1.53	1.98	1.70	2.39	2.35	2.21	1.79	1.58	1.83	2.16	1.95
$(La/Yb)_N$	6.27	4.42	6.38	6.41	4.22	2.28	7.40	5.49	3.29	6.63	6.49	5.41	5.38	3.49	6.19	6.19	5.13
Eu/Eu*	0.74	1.11	0.86	0.75	0.99	1.00	0.77	0.71	0.99	0.88	0.83	0.89	0.80	0.99	0.84	0.77	0.91

[a] Source proportions: M-GD: GD (70%), BA1 (5%), PS (15%), PL (10%); M-BA1: GD (5%), BA1 (45%), PS (40%), PL (10%); M-BA2: GD (10%), BA2 (70%), PS (5%), PL (15%); M-LT: BA2 (10%), LT (75%), PS (5%), PL (10%); M-SJ: BA2 (25%), LT (10%), SJ (60%), PL (5%).

materials were also mixed in the Barton Peninsula soils. Generally, the Patagonian dust proportion is estimated to be in the range between 5 and 15%, whereas pumice shard formed the significant contributor to the fine fraction of the soil in S-BA1 comprising ~40%. The latter contributed ~15% in S-GD, but its contribution to S-BA2, S-LT, and S-SJ is generally ~5%. The high pumice shard contribution to S-BA1 can be explained by the valley-like topography with gentle slope dipping to the southwest, the direction of the pumice shard source. This area would have been the main pathway of the southwesterly winds carrying pumice shards, which were deposited as the wind speed decelerated upslope. Other allogenic materials were sourced from neighboring bedrocks. However, this source did not play a significant role, but became locally important in soils located closed to the boundary between different bedrocks.

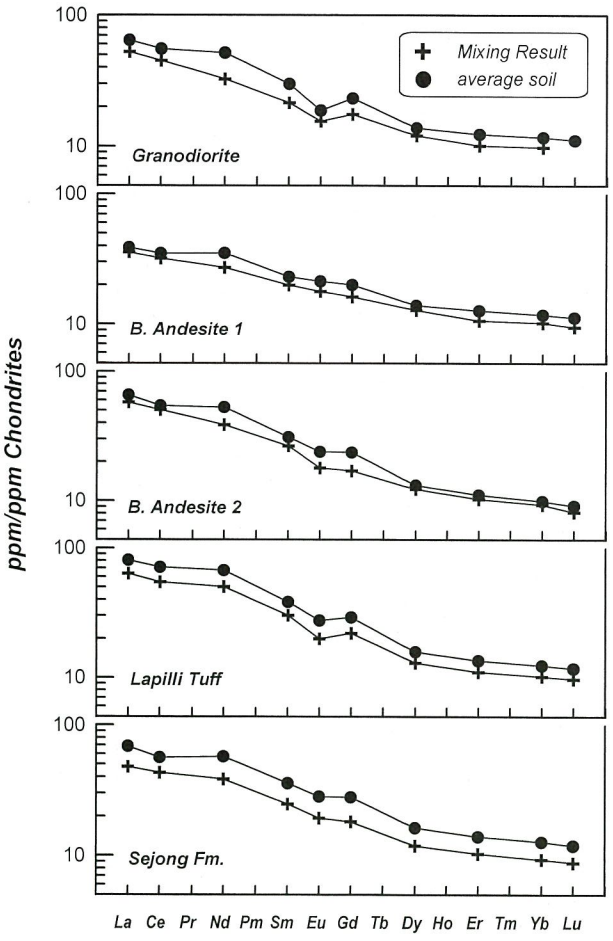

Fig. 9. Chondrite-normalized results of REE mixing calculations compared to averages of the Barton Peninsula soil suites.

7. CONCLUSIONS

Fine fractions of soils in King George Island, South Shetlands Islands, West Antarctica have been studied texturally and geochemically to understand soil-forming process. We conclude the following from the data and the discussion presented here:

1) Soils are unsorted and composed of mineral and rock fragments derived from the bedrock and volcanic ashes. The presence of both unaltered and altered pumice shards seems to indicate the importance of eolian additions to the soil formation in the Barton Peninsula, King George Island. Soils are subdivided into five suites depending on the different lithology of bedrock.

2) Chemical weathering of bedrocks on the Barton Peninsula seems insignificant based on the major elements abundances. Of the major elements, CaO is slightly depleted with respect to bedrocks except for soils developed on the Sejong Formation, the latter being very slightly enriched. In contrast, most major elements do not show any significant depletion or enrichment compared to the bedrocks. Only P_2O_5 enrichment in some soils developed on basaltic andesite and the Sejong Formation, probably due to some influence of seabirds.

3) Geochemistry of soils on the Barton Peninsula has been more influenced by eolian additions than the chemical weathering, as evidenced by rare earth element compositions. Fresh

and altered volcanic ashes blown from Deception Island contributed much in the early deglaciated areas, the western part of the peninsula, which is followed by eolian dusts sourced from Patagonia, South America. The latter influence is well distributed in the whole peninsula. Also, mixing of soil materials from the neighboring bedrocks also controlled soil REE geochemistry.

4) Even in the warmer and humid climatic conditions in the maritime Antarctic region, the chemical weathering of bedrocks seems insignificant, probably due to the relatively short time exposure of ~6000 yr since the last deglaciation. The result of this study suggests that the present soils in the maritime Antarctica are mostly composed of physically weathered mineral and rock fragments mixed with eolian additions of volcanic ashes and Patagonian dusts.

Acknowledgments—This research was supported by a grant from the Korea Ocean Research and Development Institute (PP04106) and partly by KISTEP (PN50800, PN50200). We thank Dr. G. Y. Jeong for providing some soil samples and Dr. J. L. Smellie for providing a British Antarctic Survey Scientific Report. The authors thank the 15th Korea Antarctic Research Program for logistic support. The critical reviews of Associate Editor, Dr. Martin Goldhaber and three anonymous reviewers were greatly appreciated.

Associate editor: M. B. Goldhaber

REFERENCES

Barsh D. and Mäusbacher R. (1986) New data on the relief development of the South Shetland Islands, Antarctica. *Interdisciplinary Sci. Rev.* **11,** 211–219.

Basile I., Petit J. R., Touron S., Grousset F. E. and Barkov N. (1931/2001) Volcanic layers in Atarctic (Vostok) ice cores: Source identification and atmospheric implications. *J. Geophy. Res. Atm.* **106,** 31915–3.

Basile I., Grousset F., Revel M., Petit J., Biscaye P., and Barkov N. (1997) Patagonian origin of glacial dust deposited in East Antarctica (Vostok and Dome C) during glacial stages 2, 4 and 6. *Earth Planet. Sci. Lett.* **146,** 573–589.

Beyer L., Pingpank K., Wriedt G., and Bölter M. (2000) Soil formation in coastal continental Antarctica (Wilkes Land). *Geoderma* **95,** 283–304.

Birkeland P. W. (1999) *Soils and Geomorphology* 3rd ed. Oxford University Press.

Björck S., Sandgren P., and Zale R. (1991) Late Holocene tephrochronology of the northern Antarctic Peninsula. *Quater. Res.* **36,** 322–328.

Blume H.-P., Beyer L., Bölter M., Erlenheuser H., Kalk E., Kneesch S., Pfisterer U., and Schneider D. (1997) Pedogenic zonation in soils of Southern circumpolar region. *Adv. GeoEcol.* **30,** 69–90.

Brimhall G. H. and Dietrich W. E. (1987) Constitutive mass balance relations between chemical compositions, volume, density, porosity, and strain in metasomatic hydrochemical systems: Results on weathering and pedogensis. *Geochim. Cosmochim. Acta* **51,** 567–587.

Campbell I. B. and Claridge G. G. C. (1987) *Antarctica: Soils, Weathering Processes and Environment.* Developments in Soil Sciences 16. Elsevier.

Chun H. Y., Chang S. K., and Lee J. I. (1994) Biostratigraphic study on the plant fossils from the Barton Peninsula and adjacent area. *J. Paleont. Soc. Korea* **10,** 69–84.

Claridge G. G. C. and Campbell I. B. (1977) The salts in Antarctic soils, their distribution and relationship to soil processes. *Soil Sci.* **123,** 377–384.

Condie K. C. (1991) Another look at REE in shales. *Geochim. Cosmochim. Acta* **55,** 2527–2531.

Cox R., Lowe D. R., and Cullers R. L. (1995) The influence of sediment recycling and basement composition on evolution of mudrock chemistry in the southwestern United States. *Geochim. Cosmochim. Acta* **59,** 2919–2940.

De Angelis M. and Gaudichet A. (1991) Saharan dust deposition over Mont Blanc (French Alps) during the last 30 years. *Tellus* **43B,** 61–75.

Duddy I. R. (1980) Redistribution and fractionation of rare earth and other elements in a weathering profile. *Chem. Geol.* **30,** 363–381.

Gallet S., Jahn B.-m., Van Vliet Lanöe B., Dia A., and Rossello E. (1998) Loess geochemistry and its implications for particle origin and composition of the upper continental crust. *Earth Planet. Sci. Lett.* **156,** 157–172.

Girty G. H., Marsh J., Meltzner A., McConnell J. R., Nygren D., Nygren J., Prince G. M., Randall K., Johnson D., Heitman B., and Nielsen J. (2003) Assessing changes in elemental mass as a result of chemical weathering of granodiorite in a Mediterranean (hot summer) climate. *J. Sed. Res.* **73,** 434–443.

Grousset F. E., Biscaye P. E., Revel M., Petit J. R., Pye K., Joussaume S., and Jouzel J. (1992) Antarctic (Dome C) ice core dust at 18 ky BP – isotopic constraint on origins. *Earth Planet. Sci. Lett.* **146,** 573–589.

Hamdan J. and Burnham C. P. (1996) The contribution of nutrients from parent material in three deeply weathered soils of Peninsular Malaysia. *Geoderma* **74,** 219–233.

Hall K. (1997) Rock Temperatures and Implications for Cold Region Weathering. I: New Data from Viking Valley, Alexander Island, Antactica. *Permafrost Periglacial Proc.* **8,** 69–90.

Hur S. D., Lee J. I., Hwang J., and Choe M. Y. (2001) K-Ar age and geochemistry of hydrothermal alteration in the Barton Peninsula, King George Island, Antarctica. *Ocean Polar Res.* **23,** 11–21.

Hwang J. and Lee J. I. (1998) Hydrothermal alteration and mineralization in the granodioritic stock of the Barton Peninsula, King George Island, Antarctica. *Econ. Environ. Geol.* **31,** 171–183.

Iriondo M. (2000) Patagonian dust in Antarctica. *Quarter. Int.* **68-71,** 83–86.

Jackson T. A. and Keller W. D. (1970) A comparative study of the role of lichens and "inorganic"processes in the chemical weathering of recent Hawaiian lava flows. *Am. J. Sci.* **269,** 446–466.

Jeong G. Y. and Yoon H. I. (2001) The origin of clay minerals in soils of King George Island, South Shetland Islands, West Antarctica, and its implications for the clay-mineral compositions of marine sediments. *J. Sed. Res.* **71,** 833–842.

Jin M. S., Lee M. S. and Kang P. C. (1989) Geology and petrology of the Barton and Weaver Peninsulas in King George Island, Antarctica, pp. 73–106. Report BSPG 00081-246-7. Korea Ocean Research and Development Institute.

Jwa Y. J. and Kim Y. (1991) Geochemistry of the volcanic rocks from Deception Island and its implication to back-arc spreading, pp. 275–303. Report BSPG 00140-400-7. Korea Ocean Research and Development Institute.

Kelly W. C. and Zumberge J. H. (1961) Weathering of a quartz diorite at Marble Point, McMurdo Sound, Antarctica. *J. Geol.* **69,** 433–446.

Keys J. R. and Williams K. (1981) Origin of crystalline, cold desert salts in the McMurdo region, Antarctica. *Geochim. Cosmochim. Acta* **45,** 2299–2309.

Kim H., Lee J. I., Choe M. Y., Cho M., Zheng X., Sang H., and Qin J. (2000) Geochronologic evidence for Early Cretaceous volcanic activity on Barton Peninsula, King George Island, Antarctica. *Polar Res.* **19,** 251–260.

Lee D. Y. (1992) Geomorphic features characterized by glacial and periglacial climate at Barton Peninsula, pp. 159–205. Report BSPG 00169-5-485-7. Korea Ocean Research and Development Institute.

Lee J. I., Hwang J., Kim H., Kang C. Y., Lee M. J., and Nagao K. (1996) Subvolcanic zoned granitic pluton in the Barton and Weaver peninsulas, King George Island, Antarctica. *Proc. NIPR Symp. Antarctic Geosci.* **9,** 76–90.

Lee B. Y., Won Y. and Oh. S. N. (1997) Meteorological characteristics at King Sejong Station, Antarctica (1988–1996), pp. 571–599. Report BSPE 97604-00-1020-7. Korea Ocean Research and Development Institute.

Lee J. I., Hur S. D., Yoo C. M., Yeo J. P., Kim H., Hwang J., Choe M. Y., Nam S. H., Kim Y., Park B.-K., Zheng X. and López-Martinez J. (2001) Explanatory text of the geologic map of Barton

and Weaver peninsulas, King George Island, Antarctica, p. 28. Korea Ocean Research and Development Institute.
Lottermoser B. G. (1990) Rare-earth element mineralisation within the Mt. Weld carbonatite laterite, Western Australia. *Lithos* **24,** 151–167.
Marsan F. A., Bain D. C., and Duthie D. M. L. (1988) Parent material uniformity and degree of weathering in a soil chronosequence, northwestern Italy. *Catena* **15,** 507–517.
Myrcha A. and Tatur A. (1991) Ecological role of the current and abandoned rookeries in the land environment of the maritime Antarctic. *Polish Polar Res.* **12,** 3–24.
Nesbitt H. W. (1979) Mobility and fractionation of rare earth elements during weathering of a granodiorite. *Nature* **279,** 206–210.
Nesbitt H. W. and Young G. M. (1982) Early Proterozoic climates and plate motions inferred from major chemistry of lutites. *Nature* **299,** 715–717.
Nesbitt H. W. and Young G. M. (1984) Prediction of some weathering trends of plutonic and volcanic rocks based upon thermodynamic and kinetic considerations. *Geochim. Cosmochim. Acta* **48,** 1523–1534.
Nesbitt H. W. and Wilson R. E. (1992) Recent chemical weathering of basalts. *Am. J. Sci.* **292,** 740–777.
Orheim O. (1972) Volcanic activity on Deception Island, South Shetland Islands. In *Antarctic Geology and Geophysics* (ed. R. J. Adie), pp. 117–120. Universitetsforlaget, Oslo.
Pankhurst R. J. and Smellie J. L. (1983) K-Ar geochronology of the South Shetland Islands, Lesser Antarctica: apparent lateral migration of Jurassic to Quaternary island arc volcanism. *Earth Planet Sci. Lett.* **66,** 214–222.
Pannewitz S., Schlensog M., Green T. G. A., Sancho L. G., and Schroeter B. (2003) Are lichens active under snow in continental Antarctica? *Oecologia* **135,** 30–38.
Park B.-K. (1989) Potassium-argon radiometric ages of volcanic and plutonic rocks from the Barton Peninsula, King George Island, Antarctica. *J. Geol. Soc. Korea* **25,** 495–497.
Park M. E. (1990) Epithermal alteration and mineralization characteristics of Barton Peninsula, King George Island, pp. 55–99. Report BSPG, 00111-317-7. Korea Ocean Research and Development Institute.
Petit J. R., Jouzel K., Raynaud D., Barkov N. I., Barnola J. M., Basile I., Bender M., Chappellaz J., Davis M., Delaygue M., Delmotte M., Kotlyakov V. M., Legrand M., Lipenkov V. Y., Lorius C., Pepin I., Ritz C., Saltzman E., and Stievenard M. (1999) Climate and atmospheric history of the past 420,000 years from the Vostok ice core, Antarctica. *Nature* **399,** 429–436.
Pickard J. (1986) *Antarctic Oasis, Terrestrial Environment and History of Vestfold Hills*. Academic Press.
Pye K. (1987) *Aeolian Dust and Dust Deposition*. Academic Press.
Rea D. K., Leinen M., and Janeccek T. R. (1985) Geologic approach to the long-term history of atmospheric circulation. *Science* **227,** 721–725.
Reheis M. C. (1990) Influence of climate and eolian dust on the major-element chemistry and clay mineralogy of soils in the northern Bighorn Basin, USA. *Catena* **17,** 219–248.
Schatz A. (1963) Chelation in nutrition, soil microorganisms and soil chelation. The pedogenic action of lichens and lichen acids. *J. Agri. Food Chem.* **11,** 112–118.
Seppelt R. D. and Broady P. A. (1988) Antarctic terrestrial ecosystems: The Vestfold Hills in context. *Hydrobiologia* **165,** 177–184.
Simonson R. W. (1995) Airborne dust and its significance to soils. *Geoderma* **65,** 1–43.
Smellie J. L., Pankhurst R. J., Thomson M. R. A. and Davies R. E. S. (1984) The geology of the South Shetland Islands: VI. Stratigraphy, geochemistry and evolution. Scientific Report 87. British Antarctic Survey.
Sugden D. E. and Clapperton C. M. (1986) Glacial history of the Antarctic Peninsula and South Georgia. *South Afr. J. Sci.* **82,** 508–509.
Tedrow J. C. F. and Ugolini F. C. (1966) Antarctic soils. In *Antarctic Soils and Soil Forming Processes* (ed. J. C. F. Tedrow), pp. 161–177. Antarctica Research Series 8. American Geophysics Union.
Waghenbach D. and Geis K. (1989) The mineral dust record in a high altitude alpine (Colle Gnifetti, Swiss Alps). In *Paleoclimatology and Paleometerology: Modern and Past Patterns of Global Atmospheric Transport* (eds. M. Leine and M. Sarnthein), pp. 543–564. Kluwer.
Wierzchos J., Ascaso C., Sancho L. G., and Green A. (2003) Iron-rich diagenetic minerals are biomarkers of microbial activity in Antarctic rocks. *Geomicrobiol. J.* **20,** 15–24.
Yeo J. P., Lee J. I., Hur S. D. and Choi B.-G. (2004) Geochemistry of igneous rocks in Barton and Weaver peninsulas, King George Island, Antarctica: Correlation with ancient volcanic centers. *Geosci. J.* **8,** 11–25.
Yoo C. M., Choe M. Y., Jo H. R., Kim Y., and Kim K. H. (2001) Volcaniclastic sedimentation of the Sejong Formation (Late Paleocene-Eocene), Barton Peninsula, King George Island, Antarctica. *Ocean Polar Res.* **23,** 97–107.
Yoon H. I., Park B. K., Kim Y., and Kim D. (2000) Glaciomarine sedimentation and its paleoceanographic implications along the fjord margins in the South Shetland Islands, Antarctica during the last 6000 years. *Palaeogeogr. Palaeoclimat. Palaeoecol.* **157,** 189–211.
Young G. M. and Nesbitt H. W. (1998) Processes controlling the distribution of Ti and Al in weathering profiles, siliciclastic sediments and sedimentary rocks. *J. Sed. Res.* **68,** 448–455.
Zhou Z. and Fyfe W. S. (1989) Palagonitization of basaltic glass of DSDP Site 335, Leg 37: Texture, chemical composition, and mechanism of formation. *Am. Mineral.* **74,** 1045–1053.